Revised version of paper CEJ-D-15-00445.R1

Filtration of natural organic matter using ultrafiltration membranes for drinking water purposes: circular cross-flow compared with stirred dead end flow

Running title:

Filtration of natural organic matter using ultrafiltration membranes

Norazanita Shamsuddin, Diganta B Das*, Victor M Starov

Submitted for consideration and publication in

Chemical Engineering Journal

Department of Chemical Engineering, Loughborough University, LE11 3TU, UK

*Corresponding author (Email: D.B.Das@lboro.ac.uk)

Graphical abstract

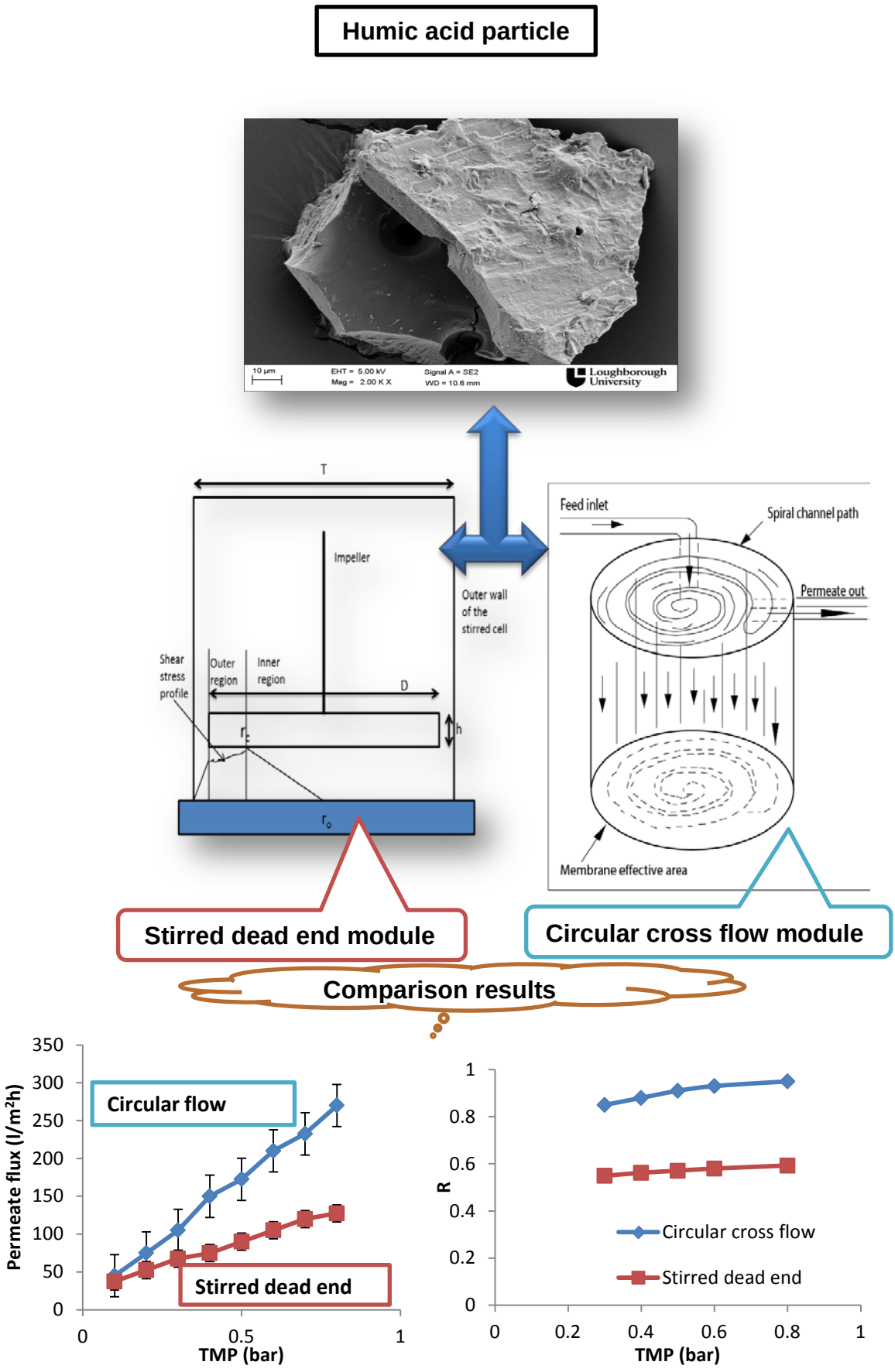

Filtration of natural organic matter using ultrafiltration membranes for drinking water purposes: circular cross-flow compared with stirred dead end flow

Norazanita Shamsuddin, Diganta B Das*, Victor M Starov

Department of Chemical Engineering, Loughborough University, LE11 3TU, UK

*Corresponding author (Email: D.B.Das@lboro.ac.uk)

Abstract

Application of ultrafiltration membranes for removal of humic acids is investigated below. Membrane filtration processes were compared using two different set-ups: circular flow and stirred dead end flow. The transmembrane pressure, temperature, feed concentration, pH, ionic strength and shear stresses applied on the membrane surfaces were kept constant whilst the permeate flux and solute rejection were measured during the experiments with both set-ups. It was shown that the rejection (both the observed and the true rejection) in the case of circular flow was higher than in the case of dead end flow. The mass transfer coefficients were determined for both set-ups. In the case of stirred dead end, it ranged in from (2.14-4.72) x 10^{-6} m/s; however, for circular cross flow system, the mass transfer coefficients were found in the range (2.24-3.22) x 10^{-5} m/s. Comparison of the mass transfer coefficients obtained for both systems showed that it was significantly higher for circular flow systems as compared with stirred dead end system at similar operating conditions. Energy consumed per volume of purified water by circular flow system (0.345 kW) was found to be much lower when by stirred dead end system (0.955 kW). This proved that the performance of circular flow system was more efficient in terms of rejection, mass transfer coefficient and energy consumption.

Key words: *Membrane filtration – ultrafiltration - circular cross flow – stirred dead end flow – mass transfer coefficient - humic acid*

Nomenclature

C_F	humic acid concentration in the feed	(kg/m^3)
C_M	humic acid concentration at the membrane surface	(kg/m^3)
C_P	humic acid concentration in the permeate	(kg/m^3)
D	diffusion coefficient	(m^2 / s)
D_t	stirred dead end cell diameter	(m)
De	Dean number	$(-)$

d_i hydraulic diameter (m)

d_c equivalent centreline diameter of curved channel (m)

h height of the impeller blade (m)

J_V volumetric flux $(m\ /\ s)$

k mass transfer coefficient $(m\ /\ s)$

L membrane channel length (μm)

Re Reynolds number $(-)$

T Operating temperature (K)

u Cross flow velocity (m/s)

Greek letters

δ momentum boundary layer $(-)$

τ shear stress (Pa)

μ dynamic viscosity $(Pa.s)$

ρ fluid density $(kg\ /\ m^3\ )$

ω angular velocity (rad/s)

1. Introduction

Clean and safe drinking water is one of the basic needs for the survival of human beings especially under extreme conditions. Regular sources of drinking water in the events of natural disasters are often polluted by harmful/hazardous components which can cause considerable losses of life. Urgent purification of polluted water under such extraordinary conditions for immediate consumption is a major priority (Chandrappa and Das, 2014). Membrane processes such as microfiltration (MF) and ultrafiltration (UF) have been widely used for water treatment in recent years (Metsämuuronen et al., 2014; Shamsuddin et al., 2014). They have been used as alternative technologies to conventional methods such as coagulation, sedimentation, ozonation, granular activated carbon (Fan et al., 2014), flocculation/chlorination (Bergamasco, 2014) and slow sand filtration (Kaiser et al., 2014) etc. The reason is that membrane processes are not only cost effective but also offer simple operation conditions, high output production with lower energy consumption and chemicals. However, one of the critical issues of membrane technology in water treatment is membrane fouling. Fouling results a considerable decline in

productivity over time and is caused by specific interactions between the membrane and the components in feed water (Shi et al., 2014; Xiao et al., 2013). Fouling results in an accumulation of colloidal matter, organic and inorganic compounds, microorganisms on membrane surfaces and within membrane pores (Lee et al., 2014; Xia et al., 2013). This is often referred to as irreversible loss of permeate flux through the membrane (Miller et al., 2014; Yamamura et al., 2014).

Various approaches for minimising membrane fouling and concentration polarization had been proposed. These include chemical methods such as modification of membrane surface to minimise interactions between the membrane and the deposits (Kochkodan et al., 2014), physical method such as mechanical scouring (Zhou et al., 2014), and hydrodynamic methods such as improved module design and fluid flow arrangements in order to reduce solute deposition on the membrane (Saxena et al., 2009). A useful method in overcoming concentration polarization is a creation of flow instabilities (Kaur and Agarwal, 2002). The use of eddies, Taylor vortices during pulsation rotating membrane filter (Charcosset, 2006) and secondary flow (Dean vortex flow) (Jaffrin, 2012) are among these options. However, the drawback of such rotating module systems is that more energy is required for scaling up and, thus they have limited large-scale development for commercial purposes. Chung et al. (1993a) and Chung et al. (1993b) studied an alternative method to create centrifugal vortices which result from the onset of unstable flow in spiral wound membrane ducts. At sufficiently low flow rates (that is at Reynolds numbers below some critical value) the velocity in the curved channel flow is approximately stream wise parabolic. However, at higher Reynolds number (or Dean number) above a critical value, centrifugal instabilities cause secondary flow containing stream wise oriented Dean vortices similar to Taylor vortices. The presence of these vortices enhance back migration through convective flow away from the membrane surface, depolarising the solute build up near the membrane surface, thus resulting in an increase of membrane permeation rate (Çulfaz et al., 2011; Moll et al., 2007; Moulin et al., 1999). Al-Bastaki and Abbas (2001) reviewed methods of improving membrane performances and reducing fouling by the presence of fluid instabilities. These techniques had proven to be successful in other applications such as gas-liquid contactors for blood oxygenation (Tanishita et al., 1975). The presence of vortices results in an improved oxygen transfer by a factor from 2 to 4 (Moulin et al., 1996). Ghogomu et al. (2001) studied the performance of several curved membrane channels designs and found that the mass transfer was improved compared to classical models. At the same time the curved channels were showed to be more energy effiecient. This was caused by the formation of Dean vortices, which proved to be effective in reducing both the concentration polarization and fouling.

It is well known that membrane module configurations can have a noticeable impact on filtration processes (Nassehi et al., 2010). However, the extent to which one system performs

better/worse under similar conditions cannot be easily quantified. Therefore, it is essential to develop conditions for comparison of the performance of different membrane systems with respect to hydrodynamics (Reynolds number, membrane surface shear, etc.) and operating conditions such as feed concentration, pH, transmembrane pressure (TMP) etc, while comparison of these different membrane systems is still possible. In order to compare two different membrane systems informative comparison has to be made with adequate experimental details provided, which were missing in some of the earlier papers, e.g., see discussions by Becht et al. (2008).

Below ultrafiltration of humic acid was studied using a stirred dead end cell (model XFUF07601; Merck Millipore, Darmstadt, Germany) and a circular flow device (Amicon, Massachusetts, USA). The transmembrane pressure, temperature, feed concentration, pH, ionic strength and shear stresses on membrane surfaces were kept constant whilst the permeate flux and percentages of solute rejection were measured during the experiments with both systems. Humic acid concentration was fixed at 30 mg/l at pH between 7 and 8 and salt concentration at 0.01M NaCl. The ultrafiltration data are compared in terms of permeate fluxes and solution rejections as well as the effects of convective mass transfer in the stirred dead end and circular flow devices. The obtained results showed noticeable differences under controlled experimental conditions. The objective is to demonstrate a significant improvement in the mass transfer coefficient and energy consumption in the case of circular flow as a result of the presence of secondary flows (Dean vortices). The TMP was kept reasonably small (less than 2 bar) in our experiments to imitate emergency situations (e.g., natural disasters) when the high pressure filtration equipment is not available and portable water filtration kits are used for drinking water purposes (Shamsuddin et al., 2014).

2. Experimental

2.1 Materials

Experiments were performed with Microdyn-Nadir (Wiesbaden, Germany) regenerated cellulose membrane (UC100: RC100) with molecular cut off (MWCO) of 100kDa and porosity of 54%. The porosity was determined using pycnometric method (Palacio et al., 1999). The membrane samples were first soaked with deionized water for one hour, water was changed every 20 minutes interval to remove any wetting agents. Membrane pore size distribution shown in Figure 1 was measured using bubble point test (Nassehi et al., 2010).

Humic acid was purchased from Sigma-Aldrich (Dorset, UK). The concentration of humic acid in the aqueous feed solution was fixed and the concentration in the permeate was evaluated. The effect of fouling was investigated at concentration of 30 mg/l of humic acid. The artificial contaminated water was prepared i.e. 30 mg of humic acid and in 1000 ml of deionized water.

The solution was mixed in an ultrasonic bath for 20 minutes to achieve a uniform distribution of humic acid in the feed. The pH was adjusted between 7 and 8. Concentrations of humic acid were evaluated spectrophotometrically using a UV spectrophotometer (model: Mini 1240 UV-VIS, Shimadzu, Milton Keynes, UK) with the absorbance measured at 254 nm. The overall humic acid concentration was determined by comparison of the absorbance data with an appropriate calibration curve. The particle size distribution of particles of humic acid was evaluated using a laser light scattering instrument for particle size determination (Malvern Instruments, Malvern, UK) and the result is presented in Figure 2 at pH between 7 and 8.

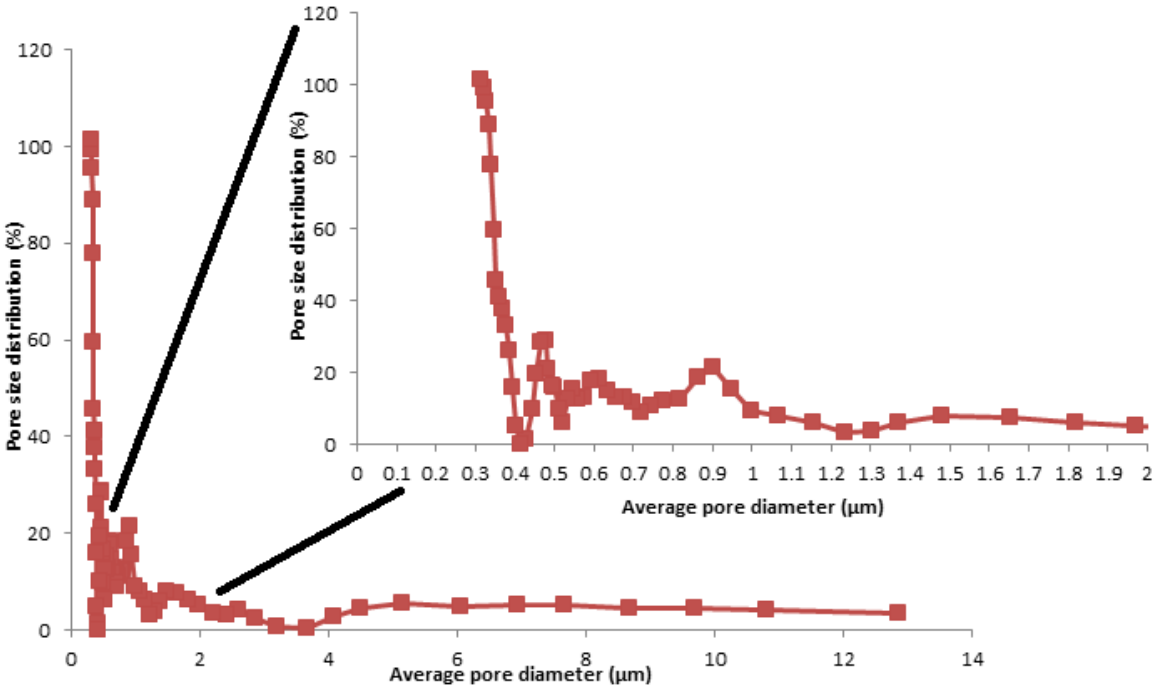

Figure 1 Pore size distribution of regenerated cellulose (RC) membrane used in this study.

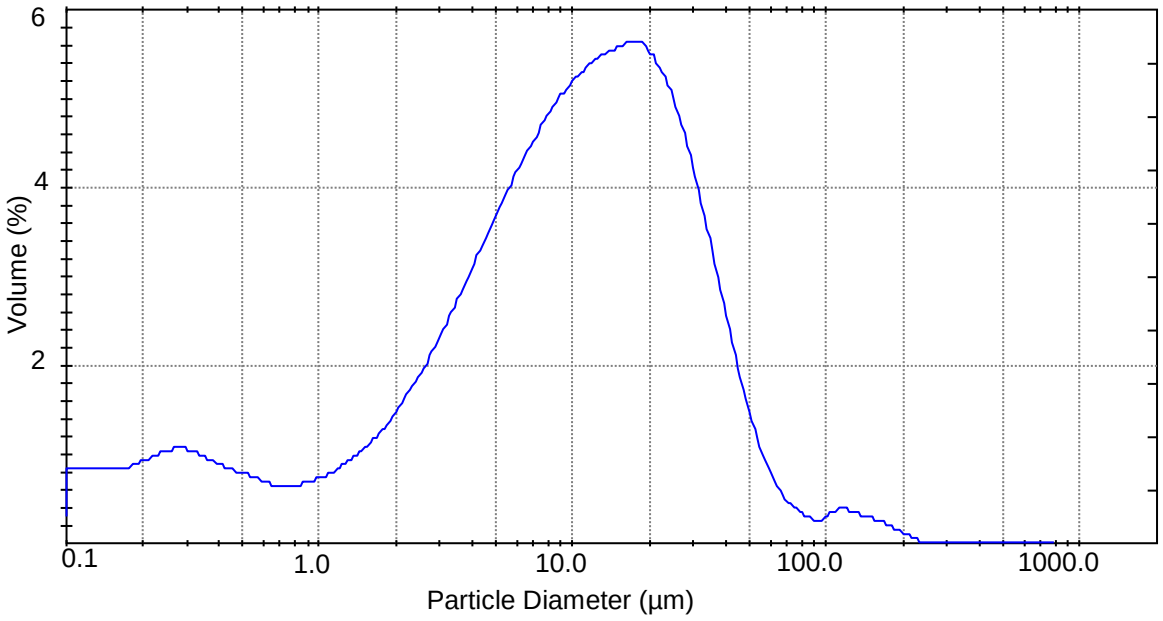

Figure 2 Size distributions of particles of humic acid in solution.

144 **2.2 Membrane filtration set-ups**

145 Two membrane configurations used are shown in Figure 3: circular cross flow systems (Figure
146 3 (a)) and the stirred dead end (Figure 3 (b)).

147 A 600 ml circular cross flow filtration cell (Amicon, Massachusetts, USA) (Figure 3 (a)) was
148 used which provides 40 cm^2 filtration surface area. The feed suspension circulated using a
149 peristaltic pump (Watson-Marlow Ltd, Cornwall, UK) in the range 83-250 ml/min. The retentate
150 was recovered and recycled back into the feed reservoir at room temperature. The suspension
151 was pumped in a circular channel over the membrane. The channel consists of three spirals of
152 varying radii from 1 cm to 4.1 cm (Figure 3 (a)) with the channel spacing approximately 1 cm.
153 The spiral channel has a width of 9.5 mm, height of 0.38 mm and length of 760 mm. The
154 pressure inside the vessel was adjusted to a predetermined inlet pressure.

155 A stirred dead end filtration Figure 3 (b) cell (Merck Milipore, Darmstadt, Germany) with a
156 diameter of 76 mm and an effective membrane area of 40 cm^2 was used. The flat blade paddle
157 impeller has a height of 9 mm and a diameter of 65 mm. The feed suspension was added into
158 the feed reservoir prior to the filtration process with maximum feed volume of 300 ml. The stirrer
159 speed was measured using a digital tachometer (Shenzhen Ever Good Electronic Co Ltd,
160 Shenzhen, China). Air from a compressor was supplied to a glass apparatus containing the UF
161 membrane at the bottom of the cell. The pressure in the filtration cell was monitored by a
162 pressure gauge and controlled using a pressure regulator (model 8286; Porter Instrument Co.,
163 Hatfield, USA). The pressure gauges for the stirred dead end and circular flow modules were
164 calibrated. Calibration was made by cross-checking the gauges with an accurate gauge of
165 varying pressures.

166 All experiments were conducted at a temperature of 22°C (±2°C). Each experiment was carried
167 out with new, clean membrane samples, which were pre-treated as described above. Filtration
168 experiments were conducted for 1 hour and 20 min for each module. Samples of permeate
169 were collected at regular intervals of 1 minute.

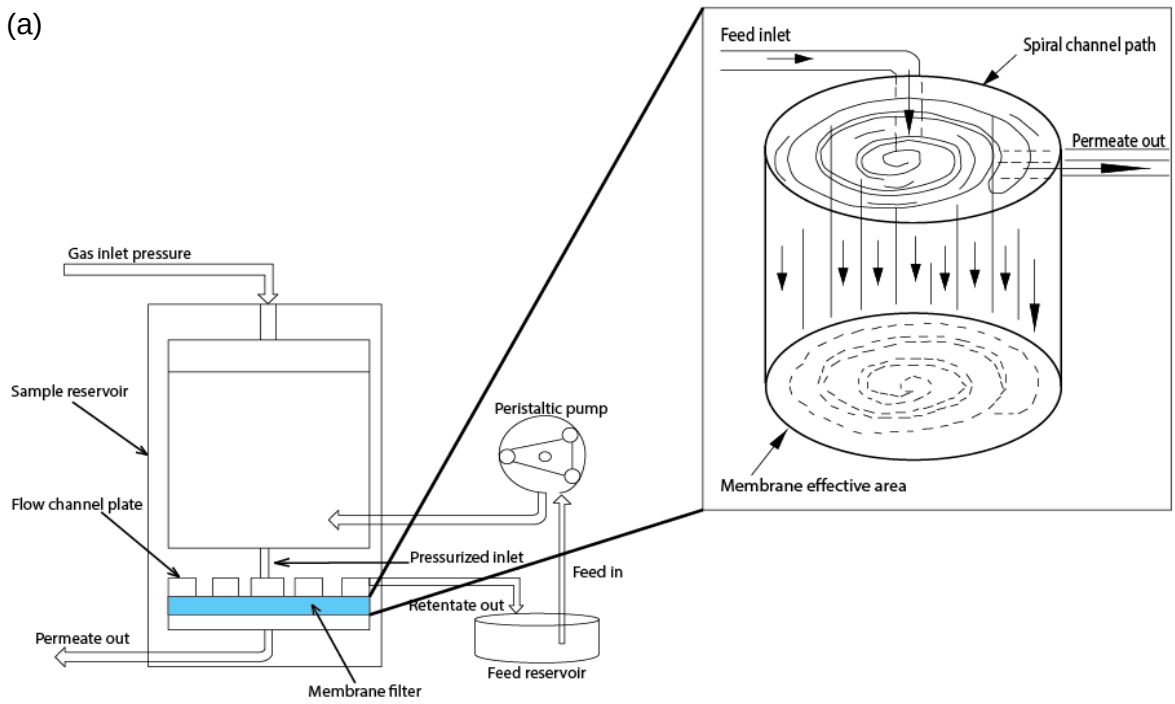

170

171 (b)

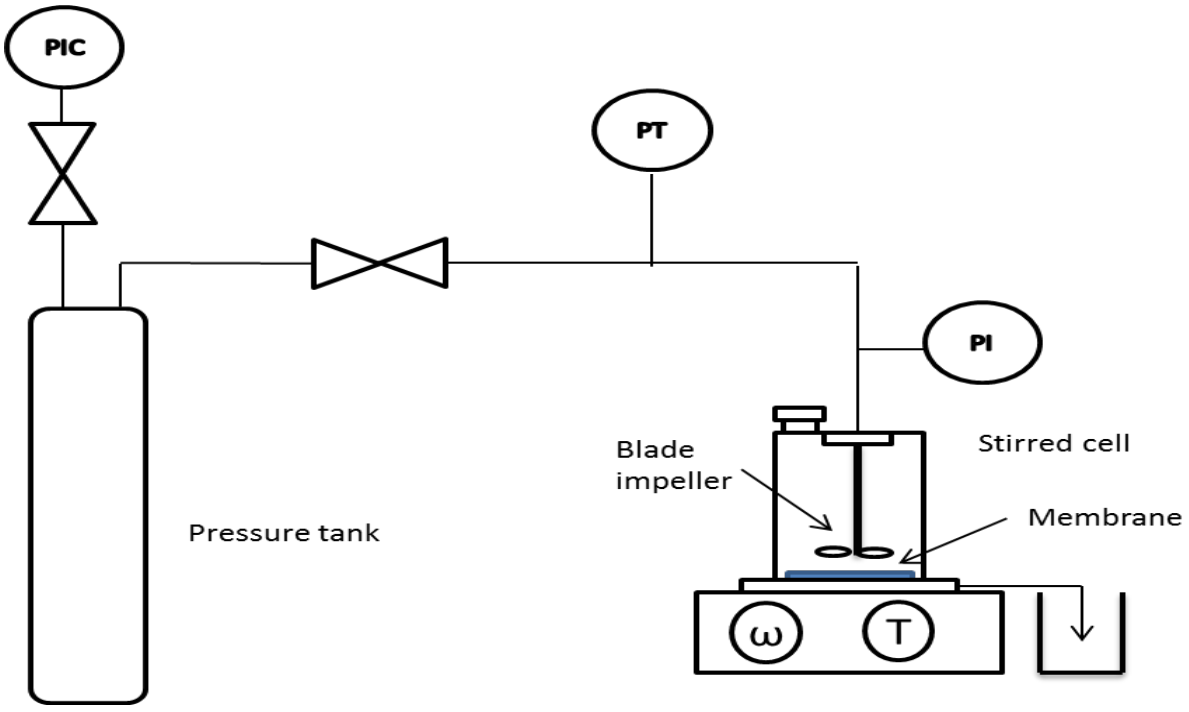

172

173 Figure 3 (a) experimental set up for circular cross flow system with a sketch of circular channel
174 path, and (b) experimental set up for stirred dead end system.

175 **2.3 Membrane thickness measurement**

176 The purpose of measuring the thickness of the membranes is to evaluate if there is any effect of
177 membrane compaction throughout the filtration processes. The measurements were carried out

by using a surface/height profiling technique. A non-contact scanning surface topography instrument, Talysurf CLI 2000 (Taylor Hobson, Leicester, UK), was used to create a profile of the membranes thickness. The membrane samples were mounted on a glass surface as a reference point. Data were collected one point at a time with each point having a discrete X, Y and Z location. A non-contact chromatic length aberration (CLA) gauge with range of 3 mm and resolution of 100 nm, and speed of 30 mm/sec was selected. For this purpose light was directed by a beam splitter through a spectral aberration lens onto the surface (that included the membrane sample). The lens then splits the light into different wavelengths and at any point on the surface only a certain wavelength was in focus. Light was reflected from the surface to a pin hole which allowed only the wavelength in focus to pass through. A spectrometer deflected the light onto a sensor to interpolate spatial position of the data point. The thickness of membrane was evaluated before and after filtration experiment for compaction.

2.4 Operating conditions of circular cross flow system

The formation of Dean vortices, which generate secondary flow perpendicular, appear in the curved channel because of the centrifugal force. If Reynolds number of the system is higher than the critical Reynolds number, when Dean vortices start to form according to Brewster et al. (1959). The critical Reynolds number can be found experimentally. Reynolds number in the circular flow system (Re_{TCF}) can be defined similar to the fluid flow in a pipe as follows:

$$Re_{TCF} = \frac{\rho u d_i}{\mu}\,, \tag{1}$$

where ρ is the density of the solution, u is the cross flow velocity of the fluid, d_i is the equivalent hydraulic diameter and μ is the dynamic viscosity of the fluid.

Dimensions of the spiral channel provided by the manufacturer are: 9.5 mm (width), 0.38 mm (height) and 760 mm (length). The peristaltic pump has a flow rate of 1.67 ml per revolution. Therefore, the rate of flow in the spiral channel can be calculated by dividing the pump flow rate with the volume of the spiral channel. Then, multiply it with the length of the spiral channel gives the cross flow velocity. The pump rotation speed of the experiments in circular cross-flow system ranged from 83-250 ml/min. Hence, the cross flow velocity was calculated in the range between 0.383 m/s to 1.156 m/s. The hydraulic diameter of the spiral channel can be calculated according to Kaur and Agarwal (2002):

$$d_i = 4\frac{Area}{Perimeter}\quad . \tag{2}$$

The hydraulic diameter equals to 0.0745 cm so the Reynolds number of the system fall in the range between 287 and 861 which lies in the laminar flow region. Dean number (De) is determined as a product of Reynolds number and the square root of the diameter ratio and

gives the ratio of the viscous force to the centrifugal force which shows the fluid motion in a curved pipe or channel:

$$De = Re_{TCF}\sqrt{\frac{d_i}{d_c}} \quad , \tag{3}$$

where d_c is the diameter of curvature of the path of the channel (equivalent centerline diameter).

The ratio of radii of the channel does not remain constant and varies in the range between 0.50 and 0.70. The equivalent centerline diameter is determined as the average radius of the channel. Therefore d_c of the circular flow system is 4.51 cm. The critical Reynolds number of our system ranges from 33 to 45 according to the data obtained in Brewster et al. (1959). The Reynolds number of our circular cross flow system is much higher than the critical Reynolds number. Therefore, Dean vortices occurred under the operating conditions implemented.

2.5 Operating conditions of the stirred dead end system

The Reynolds number of stirred dead end system is calculated as:

$$\mathrm{Re}_{SDE} = \frac{\rho\omega{r_t}^2}{\mu} \quad , \tag{4}$$

where ω is the angular velocity, and r_t is the radius of the stirred dead end system.

Reynolds number of the stirred dead end system is in the turbulent flow region that is Re ~ 77,427. In order to compare the circular cross-flow system with the stirred dead end system, all the operating conditions has to be similar. All other parameters solution concentration, pH, pressure, ionic strength and temperature of both systems were kept identical. However, the liquid mixing and the flow profile differed because there is a difference between the circular cross flow Reynolds number (laminar flow) and the rotational Reynolds number (turbulent flow). So, it has been decide to maintain similar shear stresses on the surface of the membrane in both circular cross flow system and stirred dead end system instead of keeping the identical Reynolds numbers. This allowed a direct comparison between the two systems.

The determination of the shear stress for the circular cross flow system (τ_{TCF}) is relatively easier by solving the force balance across the membrane in the circular flow system according to Becht et al. (2008):

$$\tau_{TCF} = \frac{\Delta P d_i}{4L} \quad , \tag{5}$$

where ΔP is the pressure drop across the membrane (transmembrane pressure) and L is the membrane channel length:

$$\Delta\mathrm{P} = \frac{P_i + P_o}{2} - P_p \quad , \tag{6}$$

where P_i is the inlet pressure, P_o is the outlet pressure and P_p is the permeate pressure. The shear stress across the circular cross flow membrane under operating pressure of 1 bar is approximately 12 Pa.

In order to obtain the shear stress across the membrane for the stirred dead end system, the cell was divided into two regions which were the inner and outer ones, respectively. The shear stress reaches the peak at the critical radius of the impeller and begins to decrease in the outer region. The shear stress across the membrane is the average value of that in the inner and the outer region. The critical radius of the impeller is calculated by the correlation found by Kosvintev et al. (2005) as follows:

$$r_c = \frac{D_i}{2} 1.23 \left(0.57 + 0.35 \frac{D_i}{D_t}\right) \times \left(\frac{h}{D_t}\right)^{0.036} {n_b}^{0.116} \frac{Re_d}{1000+1.43Re_d} \quad , \tag{7}$$

where D_t is the diameter of the stirred cell, D_i is the impeller diameter n_b is the number of stirred blades.

According to the definition given by Kosvintev et al. (2005) the shear stresses in the inner and outer region are determined by Eq. (8) and (9), respectively:

$$\tau_i = 0.825 \mu \omega r \frac{1}{\delta} \quad r < r_c \quad , \tag{8}$$

$$\tau_o = 0.825 \mu \omega r_c \left(\frac{r_c}{r}\right)^{0.6} \frac{1}{\delta} \quad r > r_c \quad , \tag{9}$$

where δ is the momentum boundary layer ($\delta = \sqrt{\frac{\mu}{\rho\omega}}$).

The critical radius of the stirred dead end system in our case equals to 2.37 cm. Hence, the stirrer speed is determined as 750 rpm which corresponds to the shear stress across the membrane in stirred dead end system of approximately 12 Pa. The obtained value is comparable to the value of shear stress of circular cross-flow system. Therefore, all the operating conditions are similar for both systems which give a possibility of direct and reasonable comparison between two systems.

2.6 Mass transfer coefficients for the two systems

Mass transfer coefficient quantifies the resistance to the diffusion transfer in a boundary layer at the liquid/membrane interface (Cussler, 2009), and it is an important parameter for comparing circular cross-flow system and stirred dead end system. A high value of mass transfer coefficient value means high mass transfer which is the desirable outcome. The diffusion coefficient (D) humic acid particles in the deionized water are the ratio of molar flux and the driving force for diffusion and it was determined by the Stokes-Einstein (Einstein, 1905):

$$\mathrm{D} = \frac{k_B T}{6\pi\mu r_s} \quad , \tag{10}$$

where r_s is the average radius of humic acid particles, T is the operating temperature and k_B is Boltzmann constant ($1.38 \times 10^{-23}\ m^2\ kg\ s^{-2}\ K^{-1}$). Based on the Stokes-Einstein equation, the diffusion coefficient is determined to be $1.255\ \times\ 10^{-12}\ m^2/s$.

According to the stagnant film model for concentration polarization in a membrane system (Jonsson and Boesen, 1977; Van der Berg et al., 1989; Zydney 1997) the volumetric water flux, J_V , can be written as:

$$J_V = k\ ln\left(\frac{C_M - C_P}{C_B - C_P}\right) , \tag{11}$$

where $k = D/\delta$ is the ratio of the diffusion coefficient $D$and the thickness of the concentration polarization layer, δ; C_M , C_B and C_p are the solute concentration at the membrane surface, the solute concentration in the bulk phase and the solute concentration in the permeate, correspondingly. Concentration C_M is always higher than C_B due to the concentration polarization. Eq. (11) can be rearranged as follows:

$$ln\left(\frac{1-R_{obs}}{R_{obs}}\right) = ln\left(\frac{1-R}{R}\right) + b\left(\frac{J_v}{u^a}\right) , \tag{12}$$

where $R = 1 - \frac{C_p}{C_M}$ is the true rejection and $R_{obs} = 1 - \frac{C_p}{C_B}$ is the observed rejection. The velocity variation method (Jonsson and Boesen, 1977; Van der Berg et al., 1989; Zydney 1997) is used to calculate the mass transfer coefficient for circular cross flow module. By plotting a linear relationship between $ln(1 - R_{obs})/\ R_{obs}$ vs. J_v/u^a, the true rejection R can be calculated by extrapolation to an ordinate axis, and also the value of b can be determined graphically i.e. the slope of each flux (Jonsson and Boesen, 1977; Van der Berg et al., 1989; Zydney 1997). Once R and b were found, the mass transfer coefficient, both $k_n$and k_m can be determined from Eqs. (11-12). The value $a = 0.33$ (Van der Berg et al., 1989) is used as the flow condition in the circular channel path was laminar; and $a = 0.567$ (Mehta and Zydney, 2006) is used for turbulent conditions in the stirred dead end flow system.

To convert the angular velocity (ω) for stirred dead end flow, to a linear velocity (u) in order to suit the velocity variation method, the following equation is used:

$$u = r \times \omega \ , \tag{13}$$

where r is the critical radius of the impeller i.e. 0.0237m, u is the linear velocity in m/s, and ω is the angular velocity in rad/s. The linear velocities were calculated to range between 0.390 m/s to 1.581 m/s.

3. Results and discussion

3.1 Filtration results

As stated earlier, all experiments were conducted with a humic acid at concentration 30 mg/l. The rotational Reynolds number in the stirred dead end system calculated using Eq. (4) at a stirrer speed of 750 rpm was 77,427 that the flow was turbulent. In the circular flow system the cross flow stream through the channel was laminar and the cross flow velocities were varied from 0.385 to 1.156 m/s. The Reynolds numbers (determined using Eq. (1)) for the circular flow system were in the range of 287 to 861. The shear stress at the membrane surface in both systems was approximately equal to 12 Pa according to Eq. (5-9). The maximum filtration time was 1 hour and 20 min for both systems. Since the duration of the filtration experiment was relatively short, the variation of concentration in these circumstances would not be considerable (less than 5%) over that period of time. Hence, it was possible in the first approximation to neglect this variation to simplify the calculations.

Substantial differences between the two systems were found (see Figure 5). According to Eq. (5), shear stress in the circular cross flow increases with increase in transmembrane pressures and cross flow velocities. Figure 5 (a) shows that within the range of Re number, where the flow conditions remain laminar (<1500), the observed permeation fluxes were much greater as compared to the stirred dead end system. This is due to the effects of Dean vortices, which destroy (at least partially) the concentration polarization on the membrane surface to increase, and reduces the thickness in the membrane boundary layer, improves solute mass transfer away from the membrane surface into the bulk phase.

In this work, the observed rejection (R_{obs}) was experimentally measured. However due to the concentration polarization this value is not accurate. The true concentration of solute at the membrane surface is higher than in the bulk phase, thus the real rejection was calculated using Eq. (12) using the velocity variation method (Jonsson and Boesen, 1977; Van der Berg et al., 1989; Zydney, 1997). According to the data presented in Figure 5 (b) the observed rejections (R_{obs}) for stirred dead end and the real rejections (R) were found to be low (Figure 5 (c)). Accumulation of solute on the membrane surface as a result of concentration polarization effect is likely to take place as the mass transfer coefficients calculated for the stirred dead end were significantly lower than the circular cross flow.

In the case of circular cross flow, higher R_{obs} means more solute was rejected by the membrane caused by a concentration increase in the concentration polarization layer due to higher solvent permeation and solute retention. This can be seen from Figure 5 (c) where the true rejection values in circular cross flow are higher than stirred dead end. The presence of circular channel path induces the formation of Dean vortices to disrupt rapid solute build-up on the membrane

surface by creating flow instabilities. Consequently, mass transfer coefficients of solutes away from the membrane into the bulk phase were found to be higher.

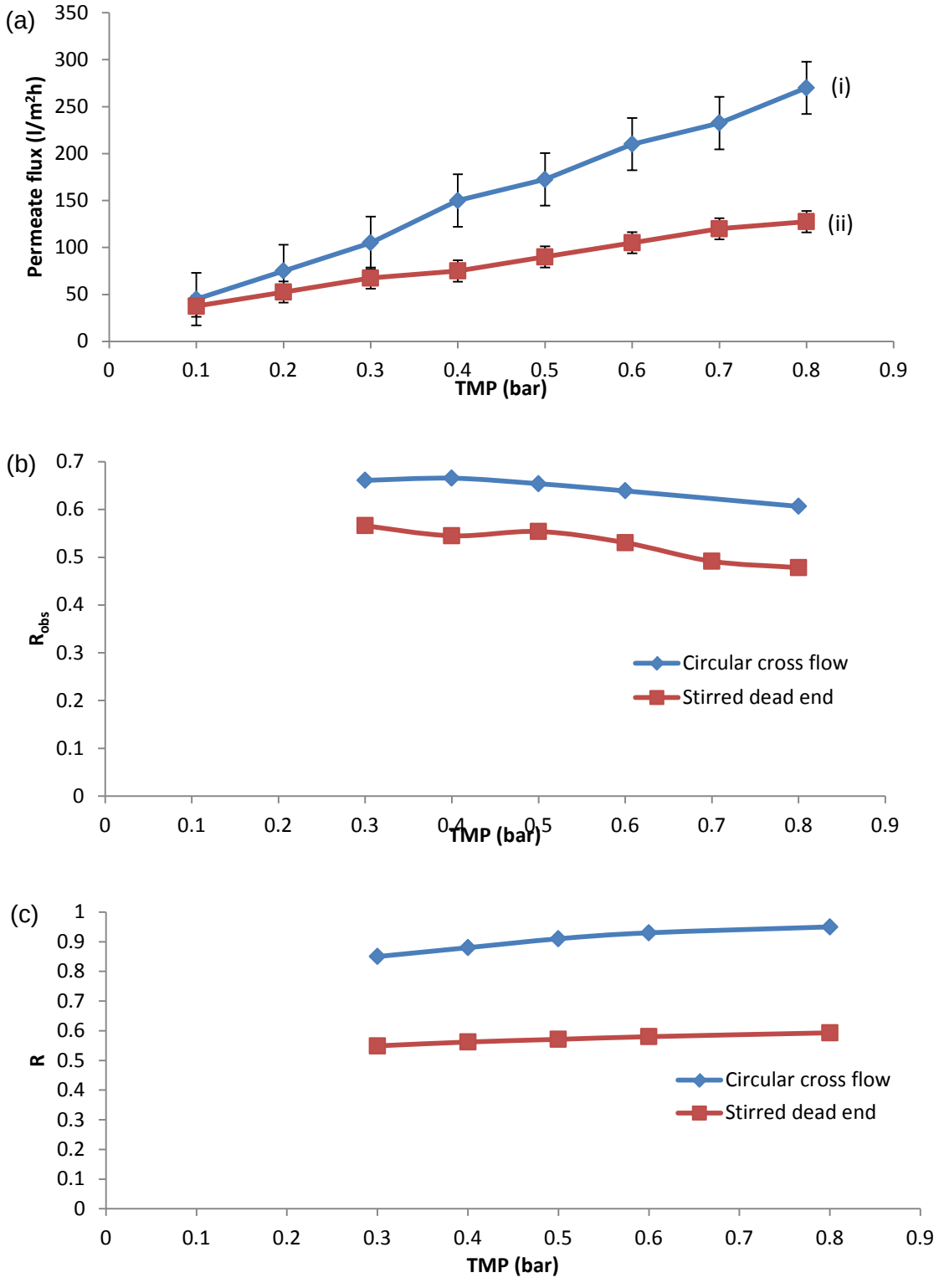

Figure 5 (a) Flux v/s TMP for both systems (i) circular cross flow, and (ii) stirred dead end, (b) effect of TMP on humic acid observed rejections (R_{obs}), (c) effect of TMP on humic acid true rejections (R) for circular cross flow system and for stirred dead end flow system.

3.2 Mass transfer coefficient

Both stirred dead end flow and circular cross flow systems, the mass transfer coefficients were determined using Eqs. (11-12). The mass transfer coefficients calculated for stirred dead end (k_n) are between (2.14-4.72) x 10^{-6} m/s. For circular cross flow system, the mass transfer coefficients (k_m) for humic acid solution calculated from our experiments fall in the range (2.24-3.22) x 10^{-5} m/s. These values are determined from data presented in Figure 6 (a-b) in which velocity variation method was used. A linear relationship was observed and all straight lines which fitted the data points showed almost identical gradient. An extrapolation to an ordinate axis will determine the value of the true rejection (R) at various pressures. According to our data the calculated values of R increased with the transmembrane pressures increase as seen in Figure 5(c).

Comparison of the mass transfer coefficients for both the systems proves that the mass transfer coefficients for circular flow systems were significantly higher as compared with stirred dead end system at similar operating conditions.

In the case of vortex flow ultrafiltration with Taylor vortices, the mass transfer coefficients were in the range of (0.4-4.0) x 10^{-5} m/s according to Agarwal (1997), whereas for cross flow filtration the mass transfer coefficients were around (1.0-5.0) x 10^{-6} m/s (Muller et al., 2003; Kaur and Agarwal, 2002). The method used by Kaur and Agarwal (2002) to assess the mass transfer coefficient is debatable as the true rejections (R) could not be extrapolated from just one crossflow velocity. This was the difference in our approach used: the velocity variation method as shown in Figure 6 (a-b) at different crossflow velocities was used, the values of mass transfer coefficients (k_m) and (k_n) and the true rejections (R) were graphically calculated. Meanwhile Figure 6 (c) shows the relationship between mass transfer coefficients (k) and TMPs for both systems. A linear relationship was expected as mass transfer would increase as TMPs increases. The values of k_m are always higher when compared with k_n at similar operating conditions, hence we conclude that circular cross flow system is better than stirred dead end.

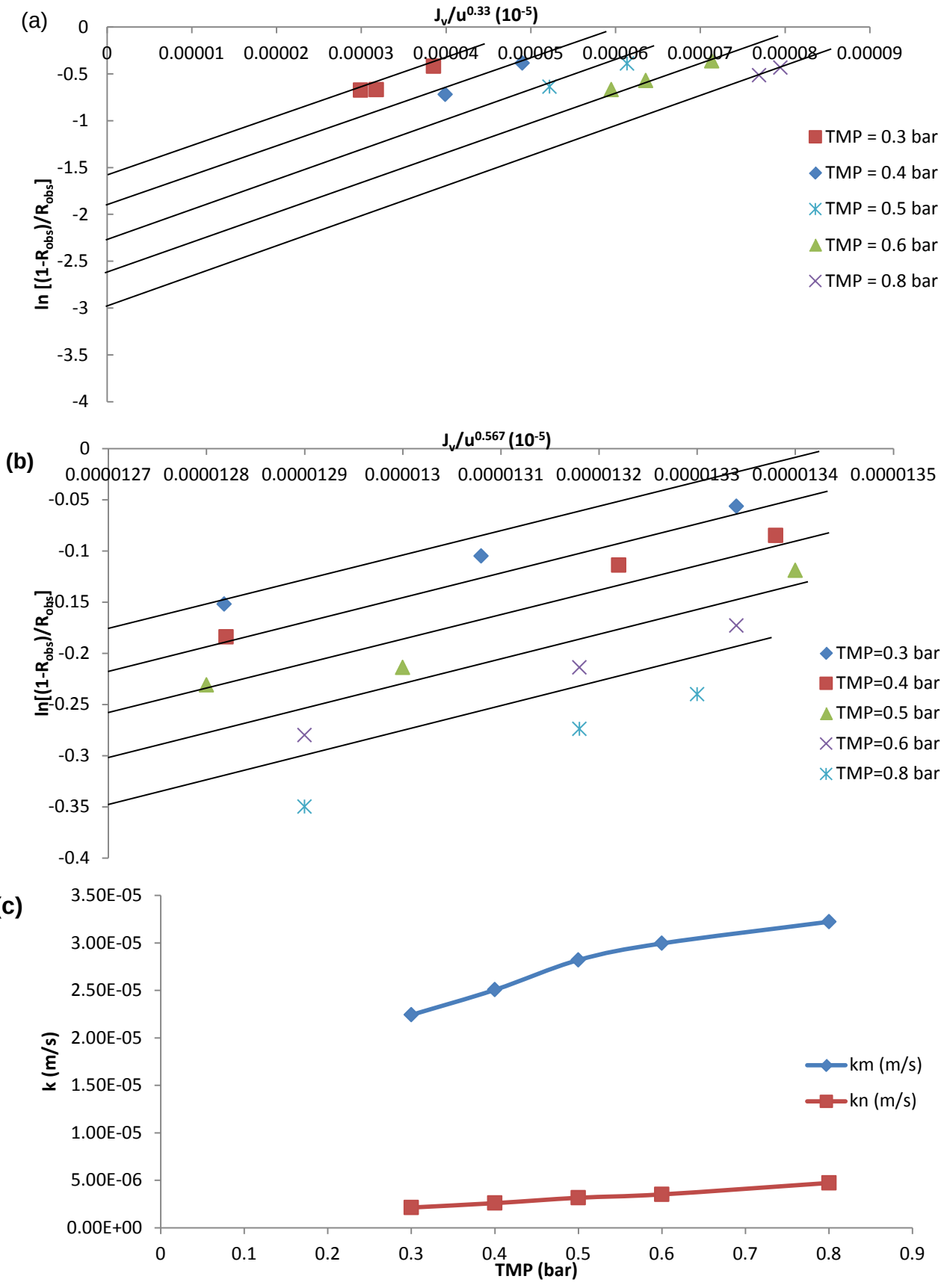

Figure 6 Velocity variation plot for (a) circular cross flow system, and (b) stirred dead end flow system, ln [(1-R_{obs})/ R_{obs}] as a function of $J_v/u^{0.33}$ and $J_v/u^{0.567}$ respectively, at various transmembrane pressures, (c) mass transfer coefficient, k_m and k_n against TMPs.

3.3 Membrane thickness measurements

Table 1 shows the membrane thicknesses and permeate qualities for both systems before and after filtration experiments. An increase in the membrane thickness less than 0.2% could be due the deposition of humic acid particles on the membrane surface but it is not significant enough to cause noticeable membrane fouling. No significant fouling was observed on the surface of the membranes in both systems due to low feed concentration (~30mg/l), but traces of humic acid can be seen in permeate when experiments were conducted with the stirred dead end module.

Table 1 Comparison of membrane thickness and permeate qualities between circular flow and stirred dead end systems.

Membrane system	Membrane thickness (before)	Membrane thickness (after)	% Thickness increase/decrease for imposed conditions	Permeate turbidity (NTU)	Average humic acid concentration in permeate (mg/l)
circular flow	273.18 ±0.05 um	273.70 ±0.05 um	±0.19% Increase	0.09±0.01	1.354±0.05
Stirred dead end flow	274.35 ±0.05 um	274.91 ±0.05 um	±0.20% Increase	0.17±0.05	13.780±0.05

Under similar operating conditions with constant TMPs of 0.5 bars for both modules, the overall permeate qualities were determined. The results shows that permeate turbidity and concentration of HA were much lower when circular flow was used. Both turbidity and humic acid concentration in permeate were less than 0.10 NTU and 2 mg/l respectively which meets the drinking water standard from WHO. In stirred dead end system however, solute penetration through the membrane causes higher turbidity and humic acid concentration in the resulting permeates. It was found that 19% calculated from transmission data represents the amount of humic acid observed in the permeate as seen from Table 1. Figures 2 and 3 give indications that smaller solute size might contribute to the transmission of HA through the pores and into the permeate.

The energy consumption for both systems were calculated and compared at similar operating conditions used. For stirred dead end system, in order to produce 12 Pa of shear stress the system required stirrer speed of 750 rpm which results a Reynolds number of 77,427. Since

Reynolds number is higher than 10^4 i.e. turbulent regimes, the power number N_T is independent of the Reynolds number, and viscosity is no longer a factor to be taken into account; the following equation was used to calculate the amount of power consumption (McCabe et al., 2001):

$$P = N_T \omega^3 {D_i}^5 \rho \quad , \qquad (14)$$

where ω is angular velocity, and D_i is the diameter of the impeller.

The total energy consumption calculated was 0.955 kW per volume of purified water. Meanwhile the total energy consumption for the circular cross flow system calculated was found 0.345 kW per volume of purified water. It was assumed for calculation of energy consumption that it is proportional to pressure drop across the membrane multiplied by the flow rate of feed for 'a thin channel flow' designs according to Bird et al. (1960). This calculation proved that energy consumed by circular cross flow system was much less than by stirred dead end system. This conclusion on energy consumption by modules with Dean vortices is in line with other authors Moulin et al. (1999) and Manno et al. (1998). These authors concluded that the presence of Dean secondary flow, even at fixed amount energy dissipated would result in more permeation fluxes compared to other conventional modules.

4. Conclusions

Ultrafiltration of humic acid solutions using two different configurations (circular flow and stirred dead end set-ups) were studied and compared. Flow arrangement in both systems is considerably different and the method of comparison has been suggested, which allows comparison under similar conditions. Both systems were compared in terms of convective mass transfer in the filtration experiments, permeate fluxes, rejections and energy consumed per volume of purified water. The presence of Dean vortices in circular flow system due to the curved geometry of the channel creates flow patterns which resulted in reducing of the effects of concentration polarization and, hence, fouling in the filtration processes and higher rejection. The mass transfer coefficients for stirred dead end system, (k_n) were determined to range from (2.14-4.72) x 10^{-6} m/s; however, for circular cross flow system, the mass transfer coefficients (k_m) were in the range (2.24-3.22) x 10^{-5} m/s. Energy consumed per volume of purified water by circular flow system (0.345 kW) was calculated to be much lower as compared to the stirred dead end system (0.955 kW). This proved that not only the performance of circular flow system was better in terms of mass transfer coefficient, and rejections but also more energy efficient.

5. Acknowledgement

The authors gratefully acknowledge a PhD studentship awarded to Norazanita Shamsuddin by Brunei Government which made this work possible.

6. References

Agarwal, G. P. “Analysis of proteins transmission in vortex flow ultrafilter for mass transfer coefficient.” *Journal of Membrane Science 136(1)*, 1997: 141-151.

Al-Bastaki, N, and A Abbas. “Use of fluid instabilities to enhance membrane performance: a review.” *Desalination 136*, 2001: 255-262.

Becht, N.O, D.J Malik, and E.S Tarleton. “Evaluation and comparison of protein ultrafiltration test results: Dead-end stirred cell compared with a cross-flow system.” *Separation and Purification Technology, 62*, 2008: 228-239.

Bergamasco, R. “Reduction of trihalomethanes using combined process coagulation/floculation/membranes in water treatment.” *36th Symposium on Biotechnology for Fuels and Chemicals .* 2014.

Bird, R.B, W.E Steward, and E.N Lightfoot. *Transport Phenomena.* New York: Wiley, 1960.

Blatt, W.F, A Dravid, A.S Michaels, and L Nelsen. “Solute polarization and cake formation in membrane ultrafiltration: causes, consequences, and control techniques.” *Membrane Science and Technology*, 1970: 47-97.

Brewster, D.B, P Grosberg, and A.H Nissan. “The stability of viscous flow between horizontal concentric cylinders.” *Proceedings of the Royal Society of London. Series A. Mathematical and Physical Sciences 251(1264)*, 1959: 76-91.

Chandrappa, R, and D.B Das. *Sustainable Water Engineering: Theory and Practice.* John Wiley & Sons, 2014.

Charcosset, C. “Membrane processes in biotechnology: an overview.” *Biotechnology advances, 24(5)*, 2006: 482-492.

Chung, K-Y, R Bates, and G Belfort. “Dean vortices with wall flux in a curved channel membrane system. 4. Effect of vortices om permeation fluxes of suspensions in microporous membrane.” *Journal of Membrane Science 81 (1)*, 1993a: 139-150.

Chung, K-Y, W.A Edelstein, and G Belfort. “Dean vortices with wall flux in a curved channel membrane system. 6. Two dimensional magnetic resonance imaging of the velocity field in a curved impermeable slit.” *Journal of Membrane Science 81 (1-2)*, 1993b: 151-162.

Çulfaz, P.Z, M Haddad, M Wessling, and R.G.H Lammertink. “Fouling behavior of microstructured hollow fibers in cross-flow filtrations: Critical flux determination and direct visual observation of particle deposition.” *Journal of Membrane Science, 372(1)*, 2011: 210-218.

Cussler, E.L. *Diffusion: Mass Transfer in Fluid Systems.* Cambridge: Cambridge University Press., 2009.

Einstein, A. “Über die von der molekularkinetischen Theorie der Wärme geforderte Bewegung von in ruhenden Flüssigkeiten suspendierten Teilchen.” *Annalen der Physik (in German) 322 (8):* , 1905: 549-560.

Fan, X, et al. “Performance of an integrated process combining ozonation with ceramic membrane ultra-filtration for advanced treatment of drinking water.” *Desalination 335(1)*, 2014: 47-54.

Ghogomu, J.N, C Guigui, J.C Rouch, M.J Clifton, and P Aptel. “Hollow-fiber membrane module design: comparison of different curved geometries with Dean vortices.” *Journal of Membrane Science (181)*, 2001: 71.

Jaffrin, M.Y. “Hydrodynamic techniques to enhance membrane filtration.” *Annual Review of Fluid Mechanics, 44,* , 2012: 77-96.

Jonsson, G, and C.E Boesen. “Concentration polarization in a reverse osmosis test cell.” *Desalination, 21*, 1977: 1-10.

Kaiser, E, C Prasse, M Wagner, K Bröder, and T.A Ternes. “Transformation of Oxcarbazepine and Human Metabolites of Carbamazepine and Oxcarbazepine in Wastewater Treatment and Sand Filters.” *Environmental Science & Technology, 48(17)*, 2014: 10208-10216.

Kaur, J, and G.P Agarwal. “Studies of protein transmission in thin channel flow module: the role of dean vortices for improving mass transfer.” *Journal of Membrane Science 196*, 2002: 1-11.

Kochkodan, V, D.J Johnson, and N Hilal. “Polymeric membranes: Surface modification for minimizing (bio) colloidal fouling.” *Advances in colloid and interface science, 206*, 2014: 116-140.

Lee, W, H.W Lee, J.S Choi, and H.J Oh. “Effects of transmembrane pressure and ozonation on the reduction of ceramic membrane fouling during water reclamation.” *Desalination and Water Treatment, 52(4-6)*, 2014: 612-617.

Manno, P, P Moulin, J.C Rouch, M Clifton, and P Aptel. “Mass transfer improvement in helically wound hollow fibre ultrafiltration modules Yeast suspensions.” *Separation and Purification Technology, 14*, 1998: 175-182.

McCabe, W.L, J.C Smith, and P Harriott. *Unit Operations of Chemical Engineering.* New York: McGraw-Hill Companies, 2001.

Mehta, A, and A.L Zydney. “Effect of membrane charge on flow and protein transport during ultrafiltration.” *Biotechnology Progress 22(2)*, 2006: 484-492.

Metsämuuronen, S, M Sillanpää, A Bhatnagar, and M. Mänttäri. “Natural organic matter removal from drinking water by membrane technology.” *Separation & Purification Reviews* 43, no. 1 (2014): 1-61.

Miller, D.J, S Kasemset, D.R Paul, and B.D Freeman. “Comparison of membrane fouling at constant flux and constant transmembrane pressure conditions.” *Journal of Membrane Science, 454*, 2014: 505-515.

Moll, R, D Veyret, F Charbit, and P Moulin. “Dean vortices applied to membrane process: Part I. Experimental approach.” *Journal of Membrane Science, 288(1)*, 2007: 307-320.

Moulin, P, J.C Rouch, C Serra, M.J Clifton, and P Aptel. “Mass transfer improvement by secondary flows: Dean vortices in coiled tubular membranes.” *Journal of Membrane Science 114 (2)* , 1996: 235-244.

Moulin, P, P Manno, J.C Rouch, C Serra, M.J Clifton, and P Aptel. “Flux improvement by Dean vortices: ultrafiltration of colloidal suspensions and macromolecular solutions.” *Journal of Membrane Science, 156(1)*, 1999: 109-130.

Muller, C.H, G.P Agarwal, Th Melin, and Th Wintgens. “Study of ultrafiltration of a single and binary protein solution in a thin spiral channel module.” *Journal of Membrane Science 227*, 2003: 51-69.

Nassehi, V, D.B Das, I.M.T.A Shigidi, and R.J Wakeman. “Numerical analyses of bubble point tests used for membrane characterisation: model development and experimental validation.” *Asia-Pacific Journal of Chemical Engineering*, 2010: 1-13.

Palacio, L, P Pradanos, J.I Calvo, and A Hernandez. “Porosity measurements by a gas penetration method and other techniques applied to membrane characterization.” *Thin Solid Films 348* , 1999: 22-29.

Saxena, A, B.P Tripathi, M Kumar, and V.K Shahi. “Membrane-based techniques for the separation and purification of proteins: an overview.” *Advances in colloid and interface science, 145(1)*, 2009: 1-22.

528 Shamsuddin, N, D.B Das, and V.M Starov. “Membrane-based point-of-use water treatment
529 (PoUWT) system in emergency situations.” *Separation & Purification Reviews (just*
530 *accepted). DOI:10.1080/15422119.2014.973967*, 2014.

531 Shi, X, G Tal, N.P Hankins, and V Gitis. “Fouling and cleaning of ultrafiltration membranes: A
532 review.” *Journal of Water Process Engineering, (1)*, 2014: 121-138.

533 Tanishita, K, P.D Richardson, and P.M Galletti. “Tightly wound coils of microporous tubing:
534 progress with secondary-flow blood oxygenator design.” *ASAIO Journal 21 (1)*, 1975:
535 216-223.

536 Van der Berg, G.B, I.G Racz, and C.A Smolders. “Mass transfer coefficients in cross-flow
537 ultrafiltration.” *Journal of Membrane Science, 47*, 1989: 25-51.

538 Xia, S, Y Zhou, R Ma, Y Xie, and J Chen. “Ultrafiltration of humic acid and surface water with
539 tubular ceramic membrane.” *Desalination and Water Treatment* , 2013: 1-8.

540 Xiao, F, P Xiao, W.J Zhang, and D.S Wang. “Identification of key factors affecting the organic
541 fouling on low-pressure ultrafiltration membranes.” *Journal of Membrane Science 447*,
542 2013: 144-152.

543 Yamamura, H, K Okimoto, K Kimura, and Y. Watanabe. “Hydrophilic fraction of natural organic
544 matter causing irreversible fouling of microfiltration and ultrafiltration membranes.” *Water*
545 *Research (54)*, 2014: 123-136.

546 Zhou, Z, F Meng, H Lu, Y Li, X Jia, and X He. “Simultaneous alkali supplementation and fouling
547 mitigation in membrane bioreactors by on-line NaOH backwashing.” *Journal of*
548 *Membrane Science, 457*, 2014: 120-127.

549 Zydney, A.L. “Stagnant film model for concentration polarization in membrane systems.” *Journal*
550 *of Membrane Science, 130*, 1997: 275-281.